Proceedings of the 9th U.S. National and 10th Canadian Conference on Earthquake Engineering
Compte Rendu de la 9ième Conférence Nationale Américaine et
10ième Conférence Canadienne de Génie Parasismique
July 25-29, 2010, Toronto, Ontario, Canada • Paper No 734

HYBRID SIMULATION TESTING OF A CONTROLLED ROCKING STEEL BRACED FRAME SYSTEM

Matthew Eatherton[1], Jerome Hajjar[2], Gregory Deierlein[3],
Xiang Ma[4], and Helmut Krawinkler[5]

ABSTRACT

Controlled rocking steel frames are a high performance seismic system that concentrates structural damage in replaceable fuse elements and virtually eliminates residual roof drifts after large earthquakes. A series of large-scale cyclic and hybrid simulation tests were completed at the MUST-SIM facility at the University of Illinois at Urbana-Champaign. The hybrid simulation test results validated the performance goals as the test specimen was subjected to amplified earthquake motions and included computational components representing the nonlinear hysteretic behavior of the rest of the building. A computational SDOF study, performed to investigate the self-centering ability of these types of structures in the presence of ambient building resistance, found excellent self-centering capability even when the restoring force was less than the yield capacity of the energy dissipation element.

Introduction

Controlled rocking systems for steel-framed buildings concentrate structural damage in replaceable energy dissipating fuse elements and virtually eliminate residual drift. Figure 1 highlights one possible configuration of this system, which employs the following components: (1) Steel frames that remain essentially elastic and are allowed to rock about the column bases. As shown in Fig. 1, the specially designed column base details permit column uplift and restrain horizontal motion by bumpers or an armored foundation trough. The configuration in Fig. 1 uses two side-by-side frames, although alternative configurations with single frames have also been investigated (Deierlein et al. 2009). (2) Vertical post-tensioning strands provide active self-centering forces. The strands are initially stressed to less than half of their ultimate strength, so as to permit additional elastic straining when the frames rock. The configuration in Fig. 1 employs post-tensioning down the center of the frame; other configurations with strands oriented on the column lines are also feasible (Roke et al. 2009). (3) Replaceable energy dissipating elements act as structural fuses that yield, effectively limiting the forces imposed on the rest of the structure. In Fig. 1, the fuses are configured as yielding shear elements between the two frames. Other configurations include fuses at the column bases or in inelastic vertical anchors. A number of different types of shear fuses were tested in this work.

[1]Graduate Research Assistant, Dept. of Civil and Env. Eng, Univ. of Illinois at Urbana-Champaign, IL 61801
[2]Professor, Dept. of Civil and Environmental Eng, University of Illinois at Urbana-Champaign, IL 61801
[3]Professor, Dept. of Structural Engineering and Geomechanics, Stanford University, Stanford, CA 94305
[4]Graduate Research Assistant, Dept. of Structural Eng. and Geomechanics, Stanford University, Stanford, CA 94305
[5]Professor, Dept. of Structural Engineering and Geomechanics, Stanford University, Stanford, CA 94305

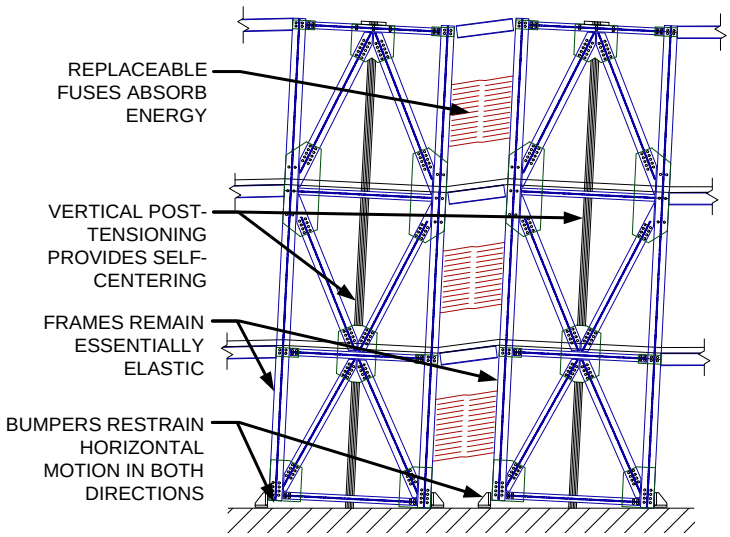

Figure 1. An example of the controlled rocking system in a dual frame configuration.

The controlled rocking system has a flag-shaped hysteretic response that is characteristic of self-centering systems. As shown in the right plot of Fig. 6, the post-tensioning force creates a bilinear elastic response in the rocking frame, as the corner of the frame is allowed to uplift. The fuse, on the other hand, typically has full hysteresis loops. The effect of combining the two elements is the flag-shaped hystersis loop shown on the left of Fig. 6.

This paper briefly summarizes the hybrid simulation testing component and related computational modeling. Other phases of this project, discussed in Hall et al. (2006), Eatherton et al. (2008), Deierlein et al. (2009), include: tests on a range of fuse topologies, finite element modeling of the fuses, a parameter study to determine key system variables, large-scale cyclic tests at the MUST-SIM facility, an SDOF study on self-centering systems including ambient building resistance, and two-thirds scale shake table tests at the E-Defense facility in Miki, Japan.

Test Configuration

The large-scale cyclic and hybrid simulation tests were conducted at the University of Illinois at Urbana-Champaign MUST-SIM facility, which is part of the George E. Brown, Jr. Network for Earthquake Engineering Simulation (NEES). The specimen, shown in Fig. 2, is based on a three story prototype building that is 36.6 m x 54.9 m (120’ x 180’) located in Los Angeles, California. The specimen design strength was calculated using an assumed response modification factor of R=8.0, four frames in each direction, and a scale factor of 0.43 relative to the prototype. A three-story braced frame was constructed using wide flange members, turned minor axis, connected using gusset plates on both sides as shown in Fig. 2. Eight 12.7 mm (½”) diameter post-tensioning strands were anchored at the roof beam and to an anchorage plate at the base that was connected to the strong floor. Steel plates with diamond shaped cut-outs served as the energy dissipating fuse and were connected to both frames (Eatherton et al. 2008). As the frames rock and one of the interior columns uplifts, the fuse is deformed in shear. The base of the frames are not attached to the base plate, instead a milled base plate with rounded bull nose edges is allowed to pivot and uplift between bumpers on all sides.

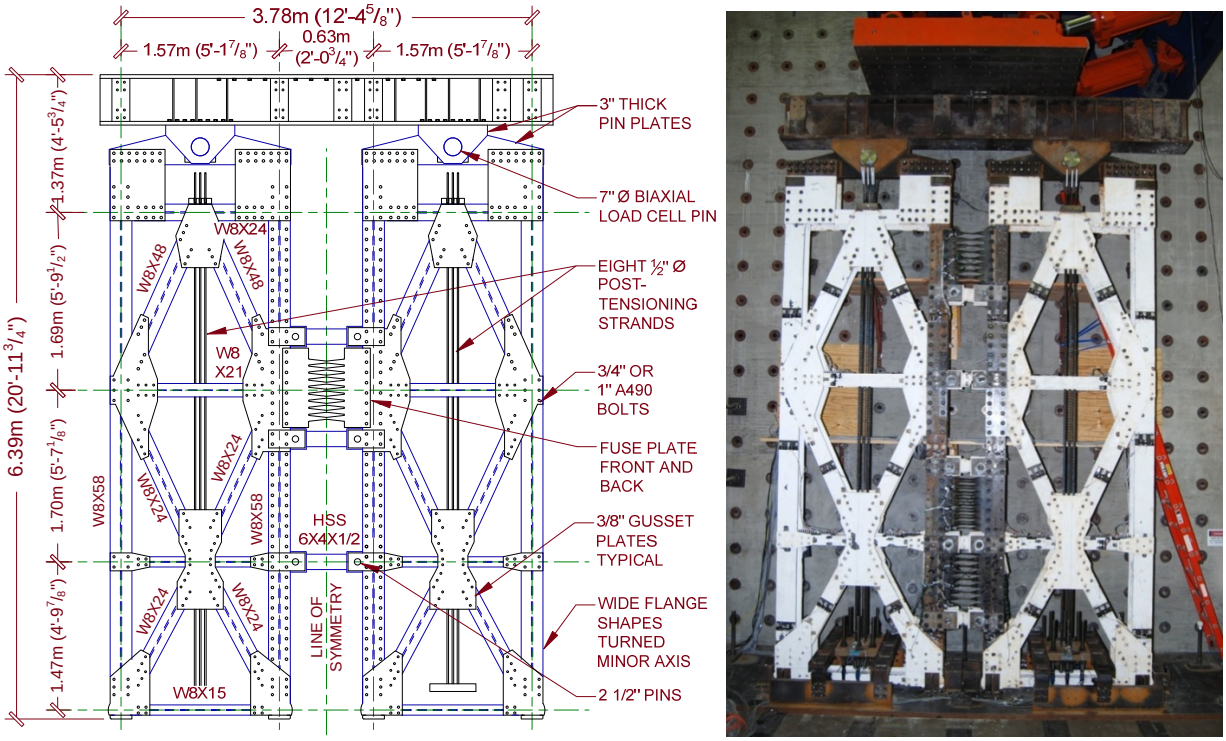

Figure 2. Diagram of the test specimen showing the Test A5 dual frame configuration (left) and photograph of the Test A6 dual frame configuration (right).

Table 1. Test program on the controlled rocking system at MUST-SIM.

Test ID	Frame Config.	Equivalent R Factor	Initial PT Stress	Fuse Configuration	Loading Protocol
A1	Dual	8.0	0.287 Fu	Six – 1/4" fuses	Quasi-Static Cyclic
A2	Dual	8.0	0.287 Fu	Two – 5/8" fuses	Quasi-Static Cyclic
A3	Dual	9.4	0.287 Fu	Two – 5/8" fuses	Quasi-Static Cyclic
A4	Dual	5.7	0.489 Fu	Two – 1" fuses	Quasi-Static Cyclic
A5	Dual	8.0	0.338 Fu	Two – 5/8" fuses	Quasi-Static Hybrid Sim.
A6	Dual	7.5	0.338 Fu	Six – 1/4" fuses	Quasi-Static Hybrid Sim.
A7	Dual	7.5	0.338 Fu	Six – 1/4" fuses	Quasi-Static Cyclic
B1	Single	8.0	0.454 Fu	One 3/4" fuse	Quasi-Static Cyclic
B2	Single	8.0	0.454 Fu	Two 3/16" fuses each side of a plate	Quasi-Static Cyclic

Load was applied to the specimen using a Load and Boundary Condition Box (LBCB) connected to a loading beam at the top of the specimen. The loading beam was connected to the specimen through two load cell pins that measured horizontal and vertical forces input into the two frames. The vertical forces in the pins were maintained at zero force throughout the test. The displacement of the specimen was controlled using feedback from two horizontal string potentiometers at the roof level.

A summary of the tests completed at the MUST-SIM facility is provided in Table 1. Nine tests were conducted consisting of seven dual-frame configuration specimens (A series), for

which the two frames are linked together with fuses, and two single-fuse configurations (B series), in which there were no fuses between the two frames and instead the fuse was concentrated at the base of each frame allowing them to act independently. Two of the dual-frame tests, Test A5 and Test A6, were conducted as hybrid simulation tests and are the focus of this paper.

Hybrid Simulation Setup

Hybrid simulation tests were used to demonstrate the performance of the controlled rocking system subjected to real ground motions in the presence of second order gravity load effects and the resistance of the rest of the building. After the components of a building undergo inelastic deformations, they will resist the displacement required to bring the building back to its original position. Two computational models were created using the OpensSEES software (Mazzoni et. al 2009) to represent the second order effects of the gravity load, and the effect of ambient building resistance. These computational components were linked to the experimental setup using the UI-SIMCOR software (Kwon et al. 2007), as schematically demonstrated in Fig. 3. Test A5 included only one computational component that represented second order gravity effects, whereas Test A6 also included a computational component representing ambient building resistance as shown in Fig. 3.

The second order gravity effects were modeled as a pinned-base leaning column with an effective gravity load lumped at the top. The effective gravity load was found by determining the amount of force that caused the same amount of P-Δ moment as three floors of tributary gravity load. The other model simulated two of the largest contributors to ambient building resistance, namely wall partitions and simple shear beam-to-column connections. As shown in Fig. 3, the simple shear beam-to-column connections were modeled as rotational springs between the beams and columns of a one bay frame. The rotational spring was calibrated to match experimental tests conducted by Liu and Astaneh (2000) as shown in Fig. 4 (left) and amplified to represent all connections tributary to one controlled rocking frame. The partitions were represented by a nonlinear hysteretic truss element that were calibrated to match experimental tests conducted by Gad et al. (1999) as shown in Fig. 4 (right), and were similarly amplified to represent all of the tributary partitions. For the sake of simplicity, exterior partitions were assumed to have identical response to interior partitions.

The JMA Kobe ground motion, shown in Fig. 5, was used to allow more direct comparison with dynamic shake table tests performed subsequently at the E-Defense facility. The ground motion was scaled to best match the design spectrum using a least squares method over a period range of interest. The period range was selected as 0.34 sec to 2 sec, which represents the initial elastic period up to the maximum expected period calculated using the secant stiffness at peak expected drift. The design response spectrum and scaled spectrum are shown in Fig. 5. Multiple trials were conducted for both Test A5 and Test A6 including trials at the MCE level corresponding to a scale factor of 0.69 and scale factors of 1.10 and 1.20 for Test A5 and A6 respectively.

As shown in Fig. 3, a displacement, Δ, is applied to both computational components, and a displacement reduced by the length scale factor, r_L, is applied to the experimental setup. The

resulting forces are measured and summed together. The displacement for the next time step is calculated using the α-OS timestepping method (Comberscure and Pegon 1997) using the measured force, F^i, computationally applied mass, M, computationally applied damping, $\zeta=0.02$, velocity, v^i, acceleration, a^i, an elastic stiffness, K_e, and the ground acceleration, $\ddot{x}_g$.

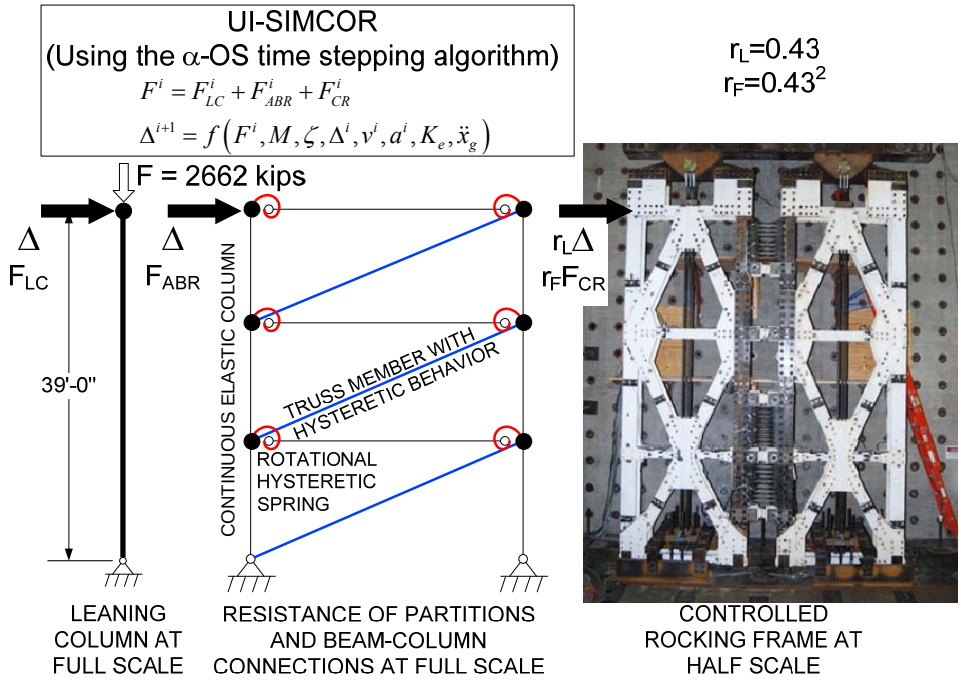

Figure 3. Schematic representation of the hybrid simulation test setup.

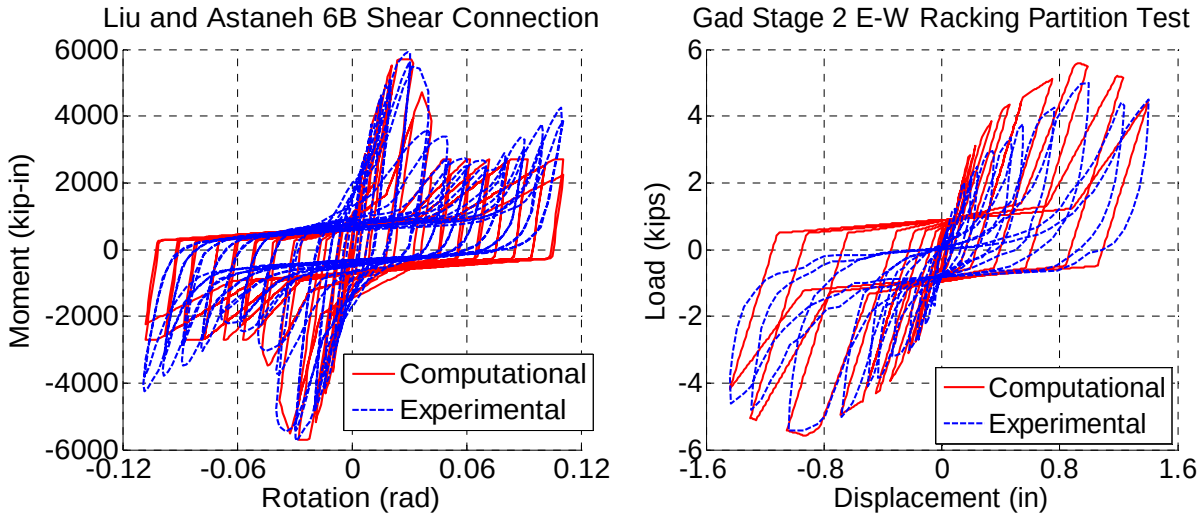

Figure 4. Calibrated simple shear beam-to-column connection response with experimental response from Test 6B Liu and Astaneh (2000) (left) and and calibrated partition response shown with experimental response from Gad et al. (1999) (right).

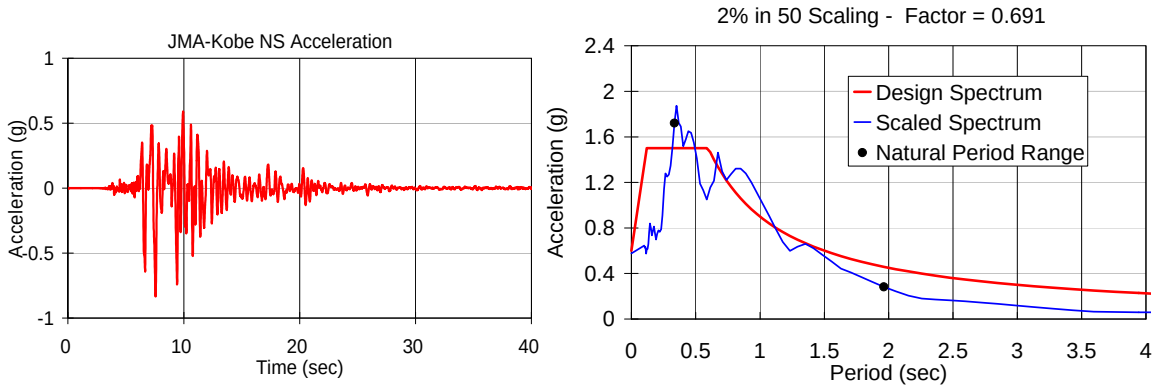

Figure 5. JMA Kobe ground motion at full scale (left) and scaling the ground motion to MCE level (right).

Computational Model of the Controlled Rocking System

A computational model of the specimen was created in the OpenSees software. The frame members were represented with elastic beam elements using a topology that matched the specimen. The frame sits on and between spring supports stiff in compression but with no stiffness in tension. The model is built in stages to simulate likely construction sequencing. The frames, supports, and post-tensioning are first created, the initial post-tension stress is then applied, and the force is allowed to equalize through the frames. Subsequently, the fuse elements are added to the model. The fuse is simulated through a component-based model in which each link is modeled using several fiber–based beam elements along the length of each link, with the depth of adjacent elements varying to match the tapered shape of the fuse links. The cyclic constitutive relationship of each fiber in the cross section discretiztion is based on an elastic-perfectly plastic stress-strain model that includes the Bauschinger effect and strain hardening. At the third points of the fuse link, rotational springs were also included to model lateral-torsional buckling of thinner fuses. This rotational spring is elastic up to a critical buckling moment, at which point the backbone degrades to represent lateral-torsional buckling. Although an elastic-plastic fuse response might be adequate to model a thicker fuse, it is necessary to simulate lateral-torsional buckling for thinner fuse plates. Using the experimental data, the computational model was refined to further capture characteristics of the fuse response, post-tensioning response, and tolerance in the pin connections.

Results and Discussion

Test A5 consisted of three trials, one at the MCE level (scale factor of 0.69), and two trials at a scale factor of 1.10 applied to the JMA Kobe ground motion. Fig. 6 shows the overturning moment-roof drift ratio response from the two latter trials with the vertical axis showing the overturning moment equal to lateral force multiplied by height divided by the calculated design overturning moment and the horizontal axis showing the roof drift ratio equal to roof displacement divided by roof height. Overturning moment is shown instead of base shear because the response is dominated by first mode rocking rather than shear related deformations. The second trial at a scale factor of 1.10 was conducted to examine possible degradation of the fuse and system. The fuse was 5/8” thick and did not experience any lateral-torsional or compression buckling, resulting in little degradation as demonstrated in the fuse hysteretic behavior shown in Fig. 7 (right) and the system response shown in Fig. 6. A slight shift in the

initial position created a small offset between the fuse and system response of the two trials.

The portions of the system response shown on the left of Fig. 6 can be decomposed into portions due to the post-tensioned steel frame and the fuse. The right side of Fig. 6 shows the portions of the system response due to each component. As shown, the post-tensioned frame creates an elastic bilinear system with self-centering but no energy dissipation. The fuse component dissipates seismic energy, but exhibits large potential residual drifts when the load is removed. Together, the flag-shaped hysteretic behavior shown on the left of Fig. 6, is capable of dissipating seismic energy and returns to near zero displacement. As shown on the left of Fig. 7, the system returns to zero displacement at the end of both trials.

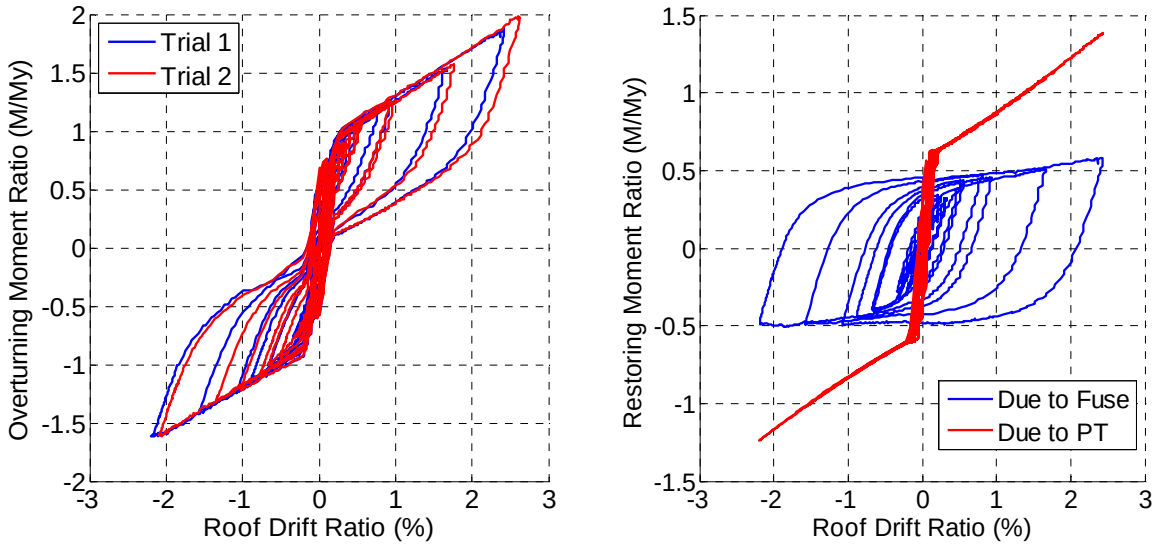

Figure 6. Load-deformation response for Test A5 during two consecutive trials at 1.10 x JMA Kobe (left) and load-deformation response due to fuse and post-tensioning separated for trial 1 at 1.10 x JMA Kobe (right).

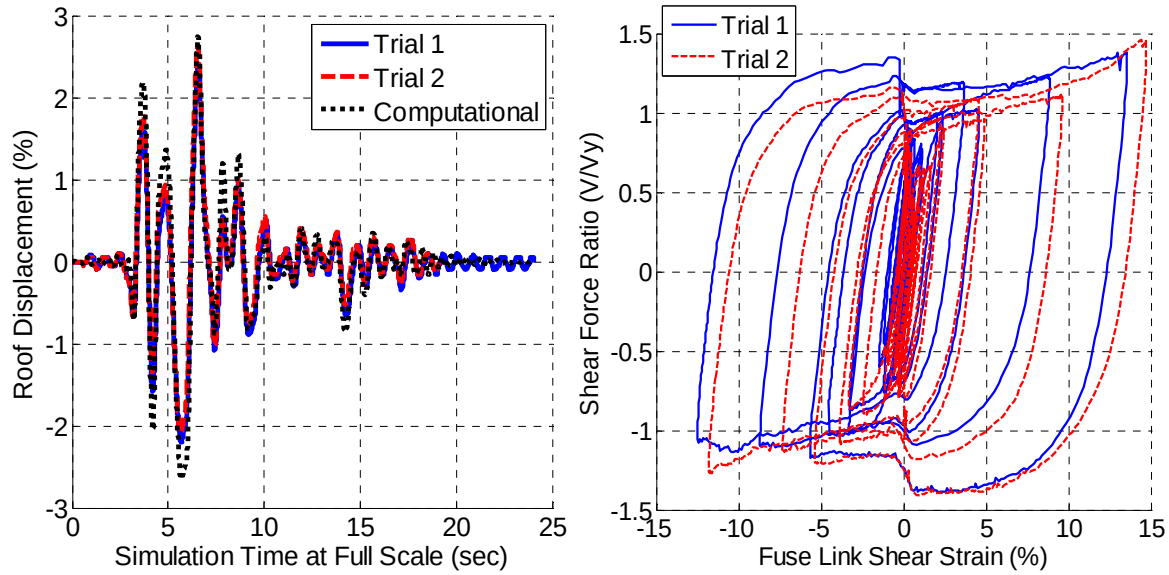

Figure 7. Displacement history for Test A5 during two consecutive trials at 1.10 x JMA Kobe (left) and fuse load-deformation response (right).

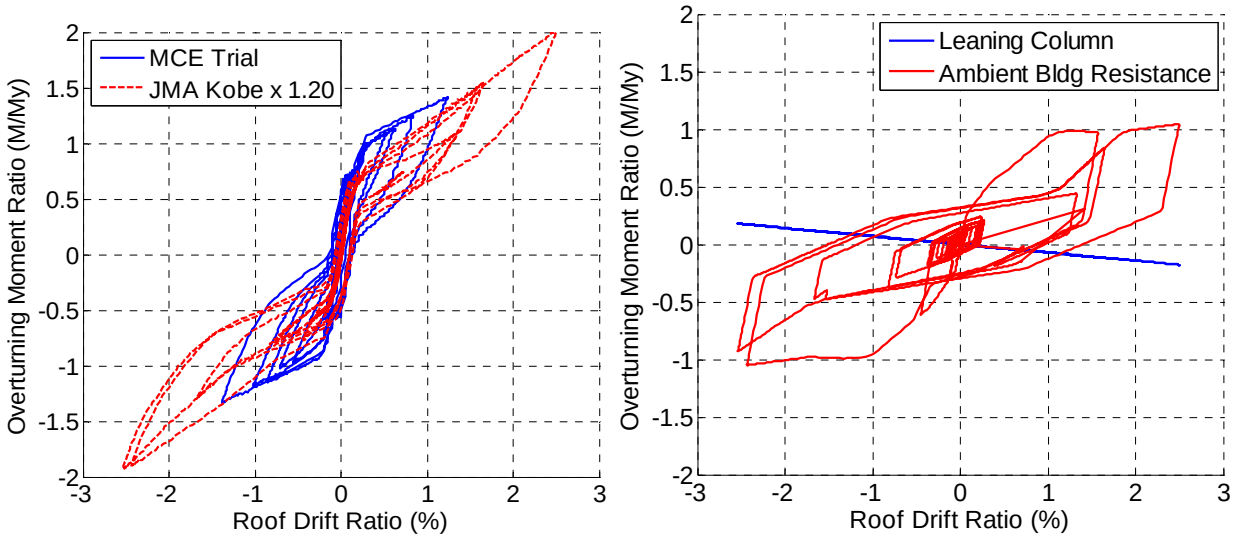

Figure 8. Load deformation response for Test A6 during two trials (left) and load-deformation response of the computational components (right).

Test A6 also consisted of three trials, one at the MCE level (scale factor of 0.69), a second at the MCE level including out-of-plane motion, and a third at a scale factor of 1.20 applied to the JMA Kobe ground motion. Test A6 used a ¼" thick fuse plate that experienced significant lateral-torsional and axial buckling during the test. As shown in Fig. 8 (left), the height of the flag-shape is taller during the MCE trial and reduces for the last trial indicating degradation in the energy dissipating component. The right side of Fig. 8 shows the response of the leaning column and the ambient building resistance computational components. The ambient building resistance produces initial resistance as large as the lateral resisting system, but then degrades leaving less resistance to self-centering as shown in Fig. 8.

Related Computational SDOF Study on Self-Centering

A related computational study investigated the residual drifts of self-centering systems including the effects of ambient building resistance (Eatherton and Hajjar 2010). Although the rest of the building is not intended or designed to resist design lateral loads, these elements typically possess sufficient lateral stiffness and strength to resist the ability of the system to self-center. Thousands of single degree-of-freedom time history analyses were analyzed representing three-story, six-story, nine-story, and twelve-story buildings subjected to 17 ground motions with a range of system variables. The idealized SDOF response is intended to simulate the response of self-centering systems in general, although it may be less representative of the response of the controlled rocking frame for some configurations (e.g., taller buildings or structures having a small restoring force relative to the energy dissipating capacity) . Fig. 9 shows an example of the results for a six-story building with horizontal force required to cause uplift, V_{iPT}, only 33% of the horizontal force corresponding to fuse yield, V_{yFuse}. The horizontal axes show partition wall density and number of tributary bays of beam column connections. Since the restoring force is less than the fuse yield capacity, it might be expected that the residual drift could be large. However, the residual drifts corresponding to the mean plus one standard deviation are small for all of the configurations shown in Fig. 9. Figure 9 demonstrates that the high levels of tributary

partitions and beam-column connections can cause reduced peak drifts and therefore slightly reduced residual drifts. Conversely, no ambient building resistance resulted in larger peak drifts and the smallest residual drifts. The parametric study concluded that for the range of ambient building resistance and configurations considered, that the restoring force only needs to be 50% as large as the yield force of the energy dissipating element to adequately control residual drifts.

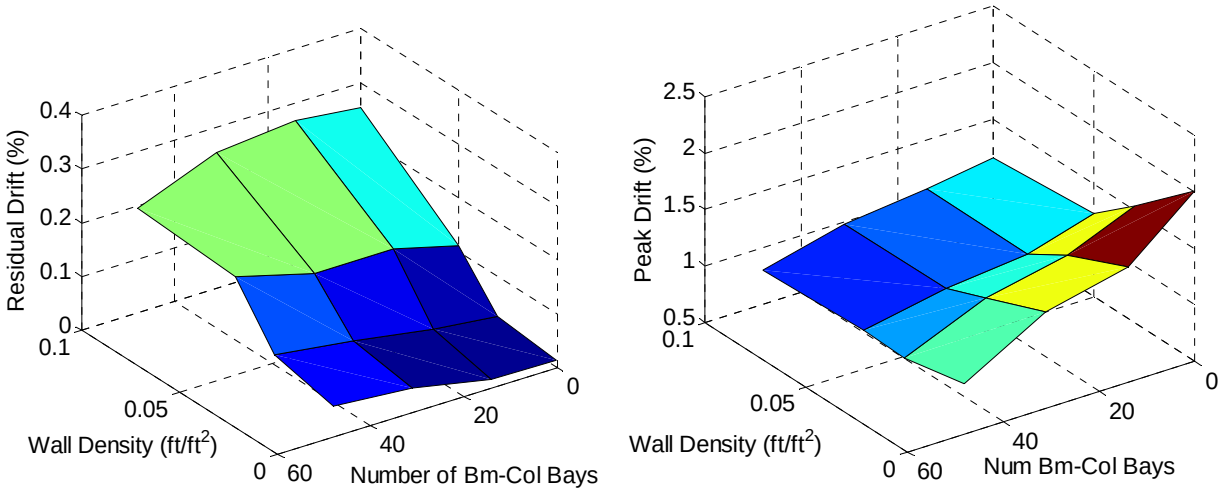

Figure 9. Representative results from a parametric SDOF study showing the mean plus one standard deviation for residual drift (left) and peak drift (right) for a six-story building with V_{iPT}/V_{yFuse}=0.33.

Conclusions

The performance of the controlled rocking system for steel-framed buildings was validated through the use of large-scale hybrid simulation testing. Residual drifts were minimal after the ground motion ceased and the frames remained elastic as the damage was concentrated in the removable fuse plates. The hybrid simulation test also demonstrated the self-centering ability in the presence of nonlinear hysteretic resistance provided by the rest of the building. A related parametric SDOF study showed that self-centering systems can control residual drifts even when the restoring force is less than the yield capacity of the energy dissipating element.

Acknowledgments

This material is based upon work supported by the National Science Foundation under Grant No. (CMMI-0530756), the American Institute of Steel Construction, Stanford University, and the University of Illinois at Urbana-Champaign. In-kind funding was provided by Tefft Bridge and Iron of Tefft, Indiana, MC Detailers of Merrillville, Indiana, Munster Steel Co. Inc. of Munster, Indiana, Infra-Metals of Marseilles, Indiana, and Textron/Flexalloy Inc. Fastener Systems Division of Indianapolis, Indiana. The authors thank graduate students, Kerry Hall, Alejandro Pena, Eric Borchers, and Paul Cordova, practicing structural engineers, David Mar and Gregory Luth, and our Japanese collaborators for their contributions to this research. The LBCB Operations Manager and LBCB Plugin used in this research were developed by Narutoshi Nakata, Matt Eatherton, Oh Sung Kwon, Sung Jig Kim, and Curtis Holub with support from NEES@UIUC, Grant No. A6000 SBC NEES OMSA-2004, and the Mid-America Earthquake

Center, NSF Grant No. EEC-9701785. Any opinions, findings, and conclusions or recommendations expressed in this material are those of the authors and do not necessarily reflect the views of the National Science Foundation or other sponsors.

References

Combescure, D. and Pegon, P. (1997). "α-Operator Splitting Time Integration Technique for Pseudodynamic Testing Error Propagation Analysis," *Soil Dynamics and Earthquake Engineering*, 16, 427-443.

Deierlein, G. G., Hajjar, J. F., Eatherton, M., Billington, S., Krawinkler, H., and Ma, X. (2009) "Seismically Resilient Steel Braced Frame Systems with Controlled Rocking and Energy Dissipating Fuses," *George E Brown Jr. Network for Earthquake Engineering Simulation (NEES) 7th Annual Meeting*, June 23-25, 2009, Honolulu, Hawaii.

Eatherton, M., Hajjar, J. F., Deierlein, G. G., Krawinkler, H., Billington, S., and Ma, X. (2008). "Controlled Rocking of Steel-Framed Buildings with Replaceable Energy-Dissipating Fuses," *Proceedings of the 14th World Conference on Earthquake Engineering*, Beijing, China, October 12-17, 2008.

Eatherton, M. and Hajjar, J. F. (2010) "Residual Drifts of Self-Centering Systems Including Effects of Ambient Building Resistance," *Earthquake Spectra*, accepted for publication.

Gad, E. F., Chandler, A. M., Duffield, C. F., and Stark, G. (1999). Lateral Behavior of Plasterboard-clad Residential Steel Frames," *Journal of Structural Engineering,* ASCE, 125(1), 32-39.

Hall, K. S., Eatherton, M., and Hajjar, J. F. (2006) *Nonlinear Behavior of Controlled Rocking Steel-Framed Building Systems with Replaceable Energy Dissipating Fuses*, UIUC Report No. ST-06-01, Department of Civil and Environmental Engineering, University of Illinois at Urbana-Champaign, Urbana, Illinois, 2006.

Kwon, O.-S., Nakata, N., Park, K.-S., Elnashai, A., and Spencer, B. (2007) *UI-SIMCOR User Manual and Examples for UI-SIMCOR v2.6 and NEES-SAM v2.0*, available from NEES Forge website: http://neesforge.nees.org/.

Liu, J., and Astaneh-Asl, A. (2000). "Cyclic Testing of Simple Connections Including Effects of Slab" *Journal of Structural Engineering,* ASCE, 126(1), 32-39.

Mazzoni, S., McKenna, F., Scott, M. H., and Fenves, G. L. (2009) *Open System for Earthquake Engineering Simulation User Command-Language Manual*, OpenSees version 2.0, Pacific Earthquake Engineering Research Center, University of California, Berkeley, CA, May.

Roke, D., Sause, R., Ricles, J. M., and Gonner, N. (2009) "Design Concepts for Damage-Free Seismic-Resistant Self-Centering Steel Concentrically Braced Frames" ASCE Structures Congress, April 30- May 2, 2009, Austin Texas.